2. S. G. Holister, Developments in Composite Materials, Applied Science Publ., London (1977).
3. R. M. Jones, Mechanics of Composite Materials, McGraw-Hill, New York (1975).
4. S. Markus, The Mechanics of Vibrations of Cylindrical Shells, Elsevier, Bratislava (1988).
5. R. D. Mindlin, "Influence of rotary inertia and shear on flexural motion of isotropic elastic plates," J. Appl. Mech., 18, 31-38 (1951).
6. S. P. Timoshenko, "The correction for shear of the differential equation for transverse vibrations of prismatic bars," Philos. Mag., 41, Ser. 6, 742-746 (1921).
7. A. Vijayaraghavan and R. M. Evan-Iwanowski, "Parametric instability of circular cylindrical shells," J. Appl. Mech., 34, 985-990 (1967).

PROPERTIES OF CHAOTIC FLUID OSCILLATIONS IN CYLINDRICAL BASINS

T. S. Krasnopol'skaya and A. Yu. Shvets

UDC 532.595:534.1

The present study is devoted to a deeper study of the properties of the chaotic interaction regimes of the oscillations of a free fluid surface in a cylindrical rigid basin and shaft rotations of a finite power electric engine, excited by spatial oscillations of the basin. The possibility and existence of such regimes were proved in [2]. In the paper mentioned, however, the proof of existence of chaotic regimes was provided only for the special case of planar oscillations of a free fluid surface. It is, therefore, necessary to investigate the possibilities of appearance of chaotic regimes in the more general case of spatial oscillations of a free surface.

Consider the mechanical system shown in Fig. 1. The crank-rod mechanism connects, on one hand, with the electric engine shaft, and, on the other, with the platform, to which is rigidly attached a cylindrical basin of radius R, partially filled by a fluid. When the crank a turns by an angle ψ, the platform acquires a displacement in the form $u(t) = a[\cos\psi + a/4\ (1 + \cos 2\psi)]$, where $a_1 = a/b$, and b is the rod length. To describe the oscillation of the free fluid surface we introduce a cylindrical coordinate system $Oxr\theta$ with origin on the shell axis at the unperturbed fluid surface. The surface equation of the free fluid surface is then written in the form $x = \eta(r, \theta, t)$. The fluid is assumed to be inviscid and incompressible with density ρ, filling a cylindrical shell of transverse cross section to a depth $x = -d$. The direction of the shell displacement $u(t)$ coincides in the cylindrical coordinate system with the direction $\theta = \theta_0$.

For the fluid velocity potential $\varphi(x, r, \theta m\ t)$ the kinematic boundary problem is written down as follows [3]:

$$\nabla^2\varphi = 0\ (-d < x < \eta;\ r,\ \theta \in S);$$

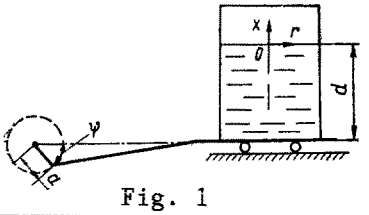

Fig. 1

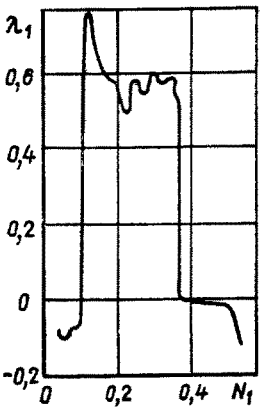

Fig. 2

Institute of Mechanics, Ukrainian Academy of Sciences, Kiev. Translated from Prikladnaya Mekhanika, Vol. 28, No. 6, pp. 52-61, June, 1992. Original article submitted February 14, 1991.

 1063-7095/92/2806-0386$12.50

$$\left.\frac{\partial\varphi}{\partial r}\right|_{r=0} < \infty; \qquad \left.\frac{\partial\varphi}{\partial r}\right|_{r=R} = 0; \qquad \left.\frac{\partial\varphi}{\partial x}\right|_{x=-d} = 0;$$
$$\frac{\partial\varphi}{\partial x} - \nabla\eta\nabla\varphi = \frac{\partial\eta}{\partial t} \quad \text{for} \quad x = \eta. \tag{1}$$

According to the Dirichlet principle (1), we obtain from the conditions [4, 7]

$$\delta I_1 = 0, \tag{2}$$

where

$$I_1 = \frac{1}{2}\int\int\int (\nabla\varphi)^2\, dSdx - \int\int (\varphi)_{x=\eta}\frac{\partial\eta}{\partial t}\, dS. \tag{3}$$

Representing η and φ in the form of series in oscillation eigenfunctions, then by [3, 7]

$$\eta(r, \theta, t) = \sum_{i,j} [q^c_{ij}(t)\,\varkappa_{ij}(r)\cos i\theta + q^s_{ij}(t)\,\varkappa_{ij}(r)\sin i\theta];$$
$$\varphi(x, r, \theta, t) = \sum_{i,j} [\varphi^c_{ij}(t)\,\chi_{ij}(x, r)\cos i\theta + \varphi^s_{ij}(t)\,\chi_{ij}(x, r)\sin i\theta], \tag{4}$$

where

$$\varkappa_{ij}(r) = N_{ij}^{-1} J_i(k_{ij}r), \quad (i = 0,1,2,\ldots;\ j = 1,2,3,\ldots);$$
$$\chi_{ij}(x, r) = \operatorname{sech}(k_{ij}d)\cdot k_{ij}(d + x)\,\varkappa_{ij}(r);$$
$$N^2_{ij} = \frac{1}{2}(1 + \delta_{0i})\left[1 - \left(\frac{i}{k_{ij}R}\right)^2\right] J_i(k_{i\ q}), \text{ [sic]} \tag{5}$$

J_e is a Bessel function, k_{ij} are the eigenvalues, determined from the equation $J'_i(k_{ij}R) = 0$; and δ_{ij} is the Kronecker symbol.

On the basis of (2) one can obtain relations of the form

$$\varphi^{c,s}_{ij}(t) = l_{ijmn}\dot{q}^{c,s}_{mn}(t), \tag{6}$$

where l_{ijmn} are nonlinear functions of the amplitudes $q^{c,s}_{0z}(t)$ [7, 8].

The kinetic energy of the fluid is then written down in the following form:

$$T = \frac{1}{2} I\dot{\psi}^2 + \frac{1}{2} m_0\dot{u}^2 + \frac{1}{2}\rho\int\int\int (\nabla\varphi)^2 dSdx = \frac{1}{2} I\dot{\psi}^2 +$$
$$+ \frac{1}{2} m_0\dot{u}^2 + \frac{1}{2}\rho S\sum_{i,j,m,n} k_{ijmn}\varphi^{c,s}_{ij}\varphi^{c,s}_{mn} = \frac{1}{2} I\dot{\psi}^2 + \frac{1}{2} m_0\dot{u}^2 + \tag{7}$$
$$+ \frac{1}{2}\rho S\sum_{i,j,m,n} a_{ijmn}\dot{q}^{c,s}_{ij}\dot{q}^{c,s}_{mn},$$

where I is the moment of inertia of the engine shaft [1], m_0 is the mass of the shell with the fluid, and k_{ijmn} and d_{ijmn} are nonlinear functions of $q^{c,s}_{0z}(t)$ [7, 8].

The displacement potential energy of the free fluid surface equals

$$V = \rho\int\int ds\int_0^\eta [\ddot{\vec{u}}\vec{y} + gx]\,dx = \rho\int\int dS\int_0^\eta [\ddot{u}(r\cos\theta_0\cos\theta + r\sin\theta_0\sin\theta) +$$
$$+ gx]\,dx = \rho S\left(\ddot{u}\sum_i r^{c,s}_{1i}q^{c,s}_{1i} + \sum_{i,j}\frac{1}{2} g q^{c,s}_{ij}q^{c,s}_{ij}\right), \tag{8}$$

where $\vec{y}$ is the displacement vector of points of the free fluid surface, g is the free fall acceleration, and

$$r^c_{1j} = \int\int r\cos\theta_0\cos^2\theta\varkappa_{1j}(r)\,dS; \qquad r^s_{ij} = \int\int r\sin\theta_0\sin^2\theta\varkappa_{1j}(r)\,dS.$$

Therefore, the system Lagrangian acquires the form ($a_1 \ll 0$)

$$L = T - V = \frac{1}{2} I\dot{\psi}^2 + \frac{1}{2} m_0 a^2 \dot{\psi}^2 \sin\psi + \frac{\rho S}{2} \sum_{i,j,m,n} a_{ijmn} \dot{q}_{ij}^{c,s} \dot{q}_{mn}^{c,s} +$$
$$+ a\rho S (\dot{\psi}^2 \cos\psi + \ddot{\psi} \sin\psi) \sum_i (r_{1i}^c q_{1i}^c + r_{1i}^s q_{1i}^s) - \frac{1}{2} \rho S g \sum_{i,j} q_{ij}^{c,s} q_{ij}^{c,s} . \tag{9}$$

The procedure of constructing the Lagrange equation makes it possible to construct the following equation for the variable $\psi(t)$

$$I\ddot{\psi} = -m_0 a^2 \psi^2 \sin\psi\cos\psi - m_0 a^2 \psi \sin\psi + a\rho S (\psi^2 \sin\psi -$$
$$- \ddot{\psi} \cos\psi)\Big(\sum_i r_{1i}^c q_{1i}^c + \sum_i r_{1i}^s q_{1i}\Big) - \quad a\rho S \dot{\psi} \cos\psi \Big(\sum_i r_{1i}^c \dot{q}_{1i}^c + \sum_i r_{1i}^s \dot{q}_{1i}^s\Big) . \tag{10}$$

On the basis of (9) one can construct the Lagrange equation for other fundamental coordinate systems, more precisely: $q_{ij}^{c,s}(t)$. The set of these equations is countable (since this is the total amount of coordinates $q_{ij}^{c,s}(t)$), therefore we introduce a simplifying assumption concerning the resonance nature of oscillations of the free fluid surface excited by the engine. Let the rotational velocity of the shaft $\dot{\psi}(t)$ in the steady regime of the engine be near the eigenfrequency ω_1 of the fundamental oscillation of the free surface, corresponding to the fundamental oscillation shapes $q^c_{11}(t)\varkappa_{11}(r)\cos\theta$ and $q^s_{11}(t)\varkappa_{11}(r)\sin\theta$. We introduce in the treatment the small positive parameter $\varepsilon = (a r_{11} k_{11}^2)^{1/3}$, where [9]

$$r_{11} = \frac{1}{2} \int_0^R r^2 \varkappa_{11}(r)\, dr = 0{,}4968\, R \text{ and } k_{11} = 1{,}8412\, R^{-1} .$$

Assuming that the conditions of resonance excitation are met, we put

$$\dot{\psi} - \omega_1 = \frac{1}{2} \varepsilon^2 \omega_1 \nu(t), \tag{11}$$

where

$$\omega_1 = (g k_{11} \operatorname{th} k_{11} d)^{1/2} .$$

The oscillations of the free fluid surface are approximated by oscillations of the fundamental and secondary shapes [9]

$$q_{01}(t)\varkappa_{01}(r); \qquad q_{21}^c(t)\varkappa_{21}(r)\cos 2\theta \text{ и } q_{21}^s(t)\varkappa_{21}(r)\sin 2\theta.$$

The amplitudes of the modes included are determined in the form

$$q_{11}^c(t) = \varepsilon\lambda [p_1(\tau)\cos\psi(t) + q_1(\tau)\sin\psi(t)];$$
$$q_{11}^s(t) = \varepsilon\lambda [p_2(\tau)\cos\psi(t) + q_2(\tau)\sin\psi(t)]; \tag{12}$$
$$q_{01}(t) = \varepsilon^2\lambda [A_{01}(\tau)\cos 2\psi(t) + B_{01}(\tau)\sin 2\psi(t) + C_{01}(\tau)];$$
$$q_{2i}^{c,s}(t) = \varepsilon^2\lambda [A_{2i}^{c,s}(\tau)\cos 2\psi(t) + B_{2i}^{c,s}(\tau)\sin 2\psi + C_{2i}^{c,s}(\tau)].$$

where $\lambda = \dfrac{\operatorname{th} k_{11} d}{k_{11}} = \dfrac{\omega_1^2}{g k_{11}}$; $\tau = \dfrac{1}{2}\varepsilon^2 \psi(t)$ is slow time, and $p_i(\tau)$, $q_i(\tau)$, $A_{ij}^{c,s}(\tau)$, $B_{ij}^{c,s}(\tau)$, $C_{ij}^{c,s}(\tau)$ are dimensionless amplitudes. To determine them we substitute (12) into the Lagrangian expression, and apply the averaging procedure over $\psi(t)$ (with fast time appearing explicitly) from 0 to 2π. As a result we obtain an expression for the averaged Lagrangian $\langle L\rangle$, from which, as shown by Whitham [4], one can obtain the averaged Lagrange equations. Restricting $B\langle L\rangle$ to terms of order $O(\varepsilon^4)$, only p_i, q_i, $dp_i/d\tau$, $dq_i/d\tau$, $\dot{\psi}$, $A_{hi}^{c,s}$, $B_{hi}^{c,s}$ and $C_{hi}^{c,s}$ appear in it, while $dA_{hi}^{c,s}/d\tau$, $dB_{hi}^{c,s}/d\tau$ and $dC_{hi}^{c,s}/d\tau$ do not. Therefore, from the equations $(\partial\langle L\rangle/\partial A_{hi}^{c,s}) = 0$; $(\partial\langle L\rangle/\partial B_{hi}^{c,s}) = 0$, $(\partial\langle L\rangle/\partial C_{hi}^{c,s}) = 0$ we determine the quantities $A_{hi}^{c,s}$, $B_{hi}^{c,s}$ and $C_{hi}^{c,s}$ as functions of $p_i(\tau)$ and $q_i(\tau)$. Following substitution of the relations obtained, $\langle L\rangle$ is written down as a function of $\dot{\psi}(t)$, $p_1(\tau)$, $q_1(\tau)$, $p_2(\tau)$ and $q_2(\tau)$ only [2]

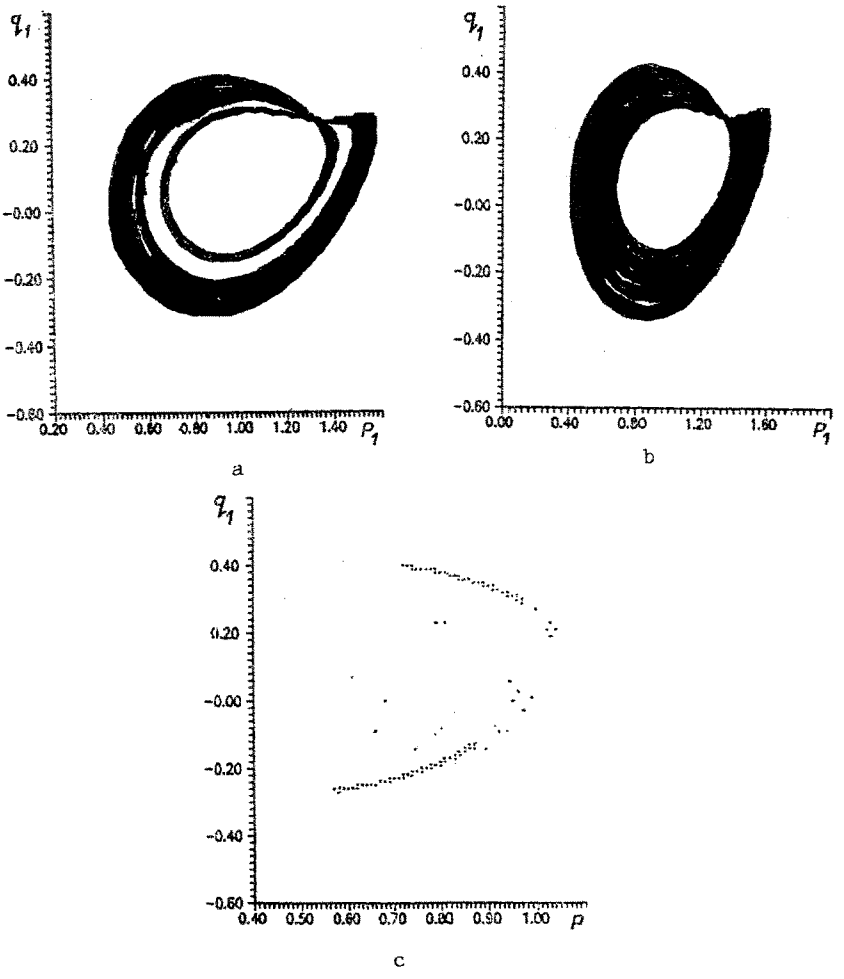

Fig. 3

$$\langle L\rangle = \frac{1}{2} I\dot{\psi}^2 + \frac{1}{4} m_0 a^2 \dot{\psi}^2 + \frac{1}{2} \varepsilon^4 g\lambda^2 \rho S\left[\frac{1}{2}\left(\frac{dp_1}{d\tau} q_1 - p_1 \frac{dq_1}{d\tau}\right) + \right.$$
$$+ \frac{1}{2}\left(\frac{dp_2}{d\tau} q_2 - p_2 \frac{dq_2}{d\tau}\right) + \gamma_0 p_1 + \frac{\gamma_1}{\omega_1^2} \ddot{\psi} q_2 + \gamma_1 p_2 + \tag{13}$$
$$\left. + \frac{\gamma_0}{\omega_1^2} \ddot{\psi} q_1 + \nu E + \frac{1}{2} AE^2 + \frac{1}{2} BM^2\right] + \varepsilon^5\{\ldots\},$$

where $\gamma_0 = \cos\theta_0$; $\gamma_1 = \sin\theta_0$; $E = E_1 + E_2$; $E_n = \frac{1}{2}(p_n + q_n)$; $M = p_1 q_2 - p_2 q_1$.

In this case E and M correspond, by eigenvectors, to the energy and angular momentum of the fluid oscillations. The constants A and B are given in [8].

We introduce a replacement of variables in the form $\psi(t) = \Omega(\tau)$, which we use following the averaging over $\psi(t)$ of the equation for the rotational coordinate of the engine shaft. As a result we have for (10)

$$\frac{d\Omega}{d\tau} = \varepsilon^2 M_2(\Omega) - \varepsilon^2 \mu_1 q_1 - \varepsilon^2 \mu_2 q_2, \tag{14}$$

where

$$\varepsilon^4 M_2(\Omega) = \frac{4[\Phi(\Omega) - H(\Omega)]}{(I + m_0 a^2)\,\omega_1}; \qquad \varepsilon^3 \mu_1 = \frac{\gamma_0 \lambda r_{11} \rho S \omega_1}{I},$$

$$\varepsilon^3 \mu_2 = \frac{\gamma_1}{\gamma_2}\ \varepsilon^3 \mu_1.$$

TABLE 1

Value of parameter N_1	Type and multiple characteristic of steady-state regime
0.05-0.099	Equilibrium position
0.1-0.1014	Limiting cycle. Onefold, period 14.375
0.1015-0.1016	Limiting cycle. Twofold, period 28.75
0.10161	Limiting cycle. Fourfold, period 57.5
0.10162	Limiting cycle. Eightfold, period 115
0.10163	Chaos. "Small" twofold
0.10164	Chaos. "Small" onefold
0.10165-0.38	Chaos. "Large"
0.38001-0.387	Limiting cycle. Twofold, period 8.75
0.388-0.524	Limiting cycle. Onefold, period 4.375
0.525	Equilibrium position

Therefore, the final closed system of Lagrange equations, describing the interaction of the oscillations of the free fluid surface and the rotation of the engine shaft, is represented on the basis of (13) and (14) in the form

$$\begin{aligned}
\frac{dp_1}{d\tau} &= -\alpha p_1 - (\nu + AE)\, q_1 - BMp_2;\\
\frac{dq_1}{d\tau} &= -\alpha q_1 + (\nu + AE)\, p_1 + BMq_2 + \gamma_0;\\
\frac{d\nu}{d\tau} &= N_3 - N_1\nu - \varepsilon\mu\gamma_0\left(q_1 + q_2\frac{\gamma_1}{\gamma_0}\right);\\
\frac{dp_2}{d\tau} &= -\alpha p_2 - (\nu + AE)\, q_2 - BMp_1;\\
\frac{dq_2}{d\tau} &= -\alpha q_2 + (\nu + AE)\, p_2 - BMq_1 + \gamma_1,
\end{aligned} \tag{15}$$

where $\varepsilon^2 M_2(\Omega) = N_0 - N_1\Omega$ is an approximation of the static characteristics of the engine, $N_3 = \frac{2}{\varepsilon^2\omega_1}[N_0 - N_1\omega_1]$; $\mu = \frac{2\mu_1}{\omega_1\gamma_0}$; $\alpha = \frac{\delta}{\omega_1}$; and δ is the coefficient of viscous damping forces $\delta\dot{q}_{11}^{c,s}$, additionally included.

The purpose of the present study is the analysis of steady-state interaction regimes. To construct solutions of the corresponding steady state regimes, as well as to determine the various quantities characterizing these regimes in the parameter space of the system of equations (15), we carried out a large number of studies of this system by means of the Personal Computer (PC) "Pyramid-286" (an IBM PC/AT 286). The basic numerical method used to construct solutions of the corresponding systems of equations is the fourth order Runge-Kutta method with a varying step correction according to Prince-Dorman. In carrying out the calculations we guaranteed a local computational accuracy of no less than $O(10^{-8})$. The construction of the Poincaré map was carried out by means of the Henon method [6]. The Lyapunov characteristic indices were constructed by the method due to Benettin et al. [5]. At the same time, the computational algorithm of the Benettin method was modified, making it possible to eliminate the effect of nontypical trajectories on the values of Lyapupnov indices. All phase portraits and Poincaré maps presented in what follows were obtained on the "Pyramid 286" PC by means of the software package GRAPHER.

As a result of the numerical experiments performed, regions of existence of steady-state chaotic regimes of the investigated systems were observed, and transition scenarios from regular to chaotic motions were analyzed.

Consider this transition in more detail. We assume that the system parameters of the system of equations (15) and the initial conditions are, respectively, equal to: $\alpha = 0.1$; $N_3 = -0.1$; $\mu = 0.5$; $\gamma_0 = 1$; $\gamma_1 = 0$, $p_1(0) = q_1(0) = \nu(0) = 0$, $p_2(0) = q_2(0) = 0.01$.

As a bifurcation parameter we consider the parameter N_1, characterizing the inclination angle of the static characteristic of an electric conductor, depending on the type of applied source of oscillation excitation.

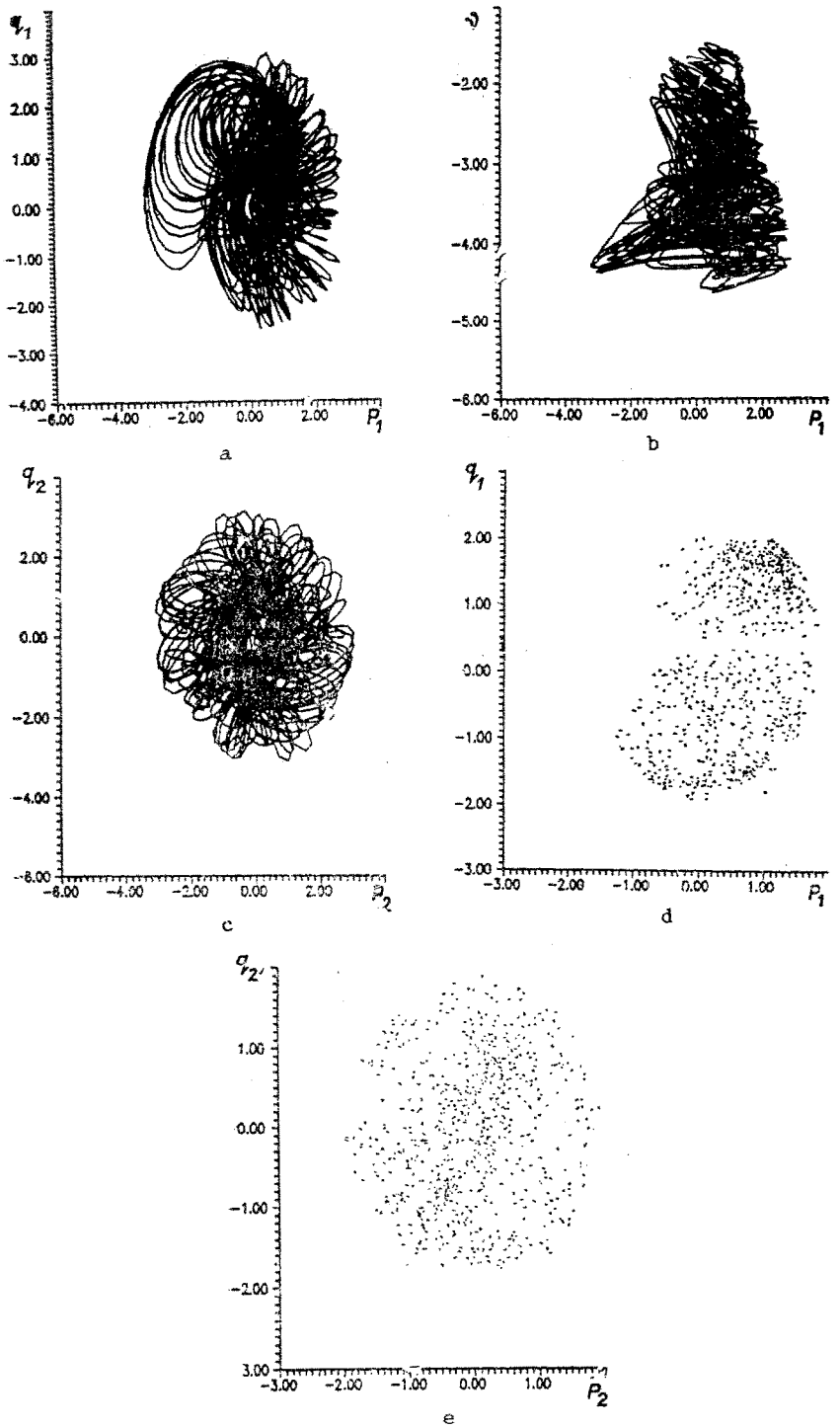

Fig. 4

As is well-known, one of the most reliable indications of the existence of a chaotic attractor is the presence in the spectrum of Lyapunov characteristic indices of system (15), of only one positive index. Figure 2 shows the leading Lyapunov index (λ_1) as a function of the parameter N_1. As seen from the figure given, there exists an interval of N_1 values, for which the λ_1 value is positive. Consequently, in this interval system (15) manifests a chaotic attractor.

Table 1 presents types of steady-state solutions of the system of equations (10) for a parameter N_1 varying from 0.05 to 0.525. We consider in more detail the bifurcations observed in the system. For $0.1 > N_1 \geq 0.05$ there exists a stable equilibrium position. At $N_1 = 0.1$ this equilibrium position loses its stability, leading to the appearance, as a result

of the Andronov–Hopf bifurcation, of a onefold limiting cycle of period 14.375. At the point $N_1 = 0.1015$, then, this limiting cycle becomes unstable, and, as a result of period doubling bifurcation, a stable twofold limiting cycle of period 28.75 is generated in the system. Further period doubling bifurcations occur in the system at the points $N_1 = 0.10161$ and $N_1 = 0.10162$, leading, respectively, to generation of fourfold and eightfold limiting cycles of periods of 57.5 and 115. A further cascade of doubling bifurcations leads to generation of a chaotic attractor at $N_1 = 0.10163$. The projection of this attractor on the (p_1q_1) plane is shown in Fig. 3a. As follows from the results obtained, the transition to chaos in the system is implemented rigorously according to the Feigenbaum scenario. A structural rearrangement of the "chaos–chaos" type is observed in the system at $N_1 = 0.10164$, as a result of which there is merging of the twofold spiral of the attractor into a onefold. The projection of this chaotic attractor spiral is shown in Fig. 3b. The Poincaré map of this chaotic attractor by the plane $\gamma = -1.55$ is shown in Fig. 3c. As seen from Fig. 3c, this map has a band structure. The major Lyapunov index of both chaotic attractors, given in Fig. 3, is approximately 0.27. We turn attention to one characteristic feature, present in all regimes shown above, both regular and chaotic. It consists of the fact that for all steady-state regimes $p_2 = q_2 = 0$, i.e., oscillations (chaotic and regular) of the free fluid surface occur only in the first form.

At $N_1 = 0.10165$ the system undergoes again a rearrangement of the "chaos–chaos" type. The chaotic attractor, shown in Fig. 3b, is changed by a chaotic attractor of a different type. The projections of this attractor (for $N_1 = 0.125$) on the planes (p_1, q_1), (p_1, ν), (p_2, q_2), respectively, are shown in Figs. 4a-c. Figures 4d-e show the projections of the Poincaré map of the given attractor by the plane $\nu = -2.5$.

Consider the main distinctions between this chaotic attractor and the chaotic attractors shown in Figs. 3a, b. Firstly, nonvanishing chaotic oscillations are generated in the second form in the variables (p_2, q_2). Secondly, the oscillation amplitudes in the variables p_1, q_1, and ν increase substantially. Thirdly, the spiral structure of the attractor disappears, and, as seen from Fig. 4, it becomes substantially more complicated. Fourthly, the band structure of the Poincaré map is lost, and these maps acquire the form of some stochastic set (Figs. 4d, e). Fifth, the value of the major Lyapunov index increases to values of the order of 0.45-0.6, i.e., the rate of dispersion of close phase trajectories increases by almost a factor of two. The chaotic nature of this type, is conditionally called "large," unlike the chaotic attractors shown in Fig. 3, called "small" in the following.

As a result of the numerical calculations performed it has been established that a "large" chaotic attractor exists in system (15) for parameter values changing from 0.10165 to 0.38. We note that the cascade of doubling bifurcations earlier investigated, as well as the generation of "small" chaos and its structural rearrangements, occur in a very small interval of variation of the parameter N_1. Thus, for varying N_1 values the region of existence of "large" chaos exceeds substantially the region of existence of "small" chaos. The projections of the chaotic attractor, constructed for $N_1 = 0.3745$, and its Poincaré map by the plane $\nu = -1$ are given, respectively, in Figs. 5a-e.

As seen from Figs. 4 and 5, the chaotic attractors constructed on the boundaries of the region of existence of "large" chaos are qualitatively identical, and only some decrease in amplitude is observed, with chaotic oscillations established for increasing N_1 values.

It must be stressed that a "large" chaotic attractor has a relatively large attractive basin. At least, for any solution of system (15), at an initial moment of time found in the region $\tilde{S}:\{|p_i| \leq 3,\ |q_i| \leq 3,\ |\nu| \leq 3,\ i = 1, 2\}$, the "large" chaotic attractor is a unique attractor, i.e., all solutions of the system of equations (10), whose initial values are found in the region $\tilde{S}$, become chaotic.

We would like to turn attention to an extremely important feature. The construction of phase portraits, Poincaré maps, and the calculation of Lyapunov indices must be carried out with a time delay relative to the initial time of the numerical calculation – one must discard a certain (not very substantial) number of the first N values of the corresponding time realization $p_i(t_k)$, $q_i(t_k)$, $\nu(t_k)$, $i = 1, 2$; $k = N + 1, N + 2, N + 3, \ldots$. The necessity of this discarding is related to the exclusion of phase portraits of steady-state regimes by trajectories of transient processes. In the opposite case chaotization of the transient process can be perceived erroneously to occur following the steady-state chaotic regime.

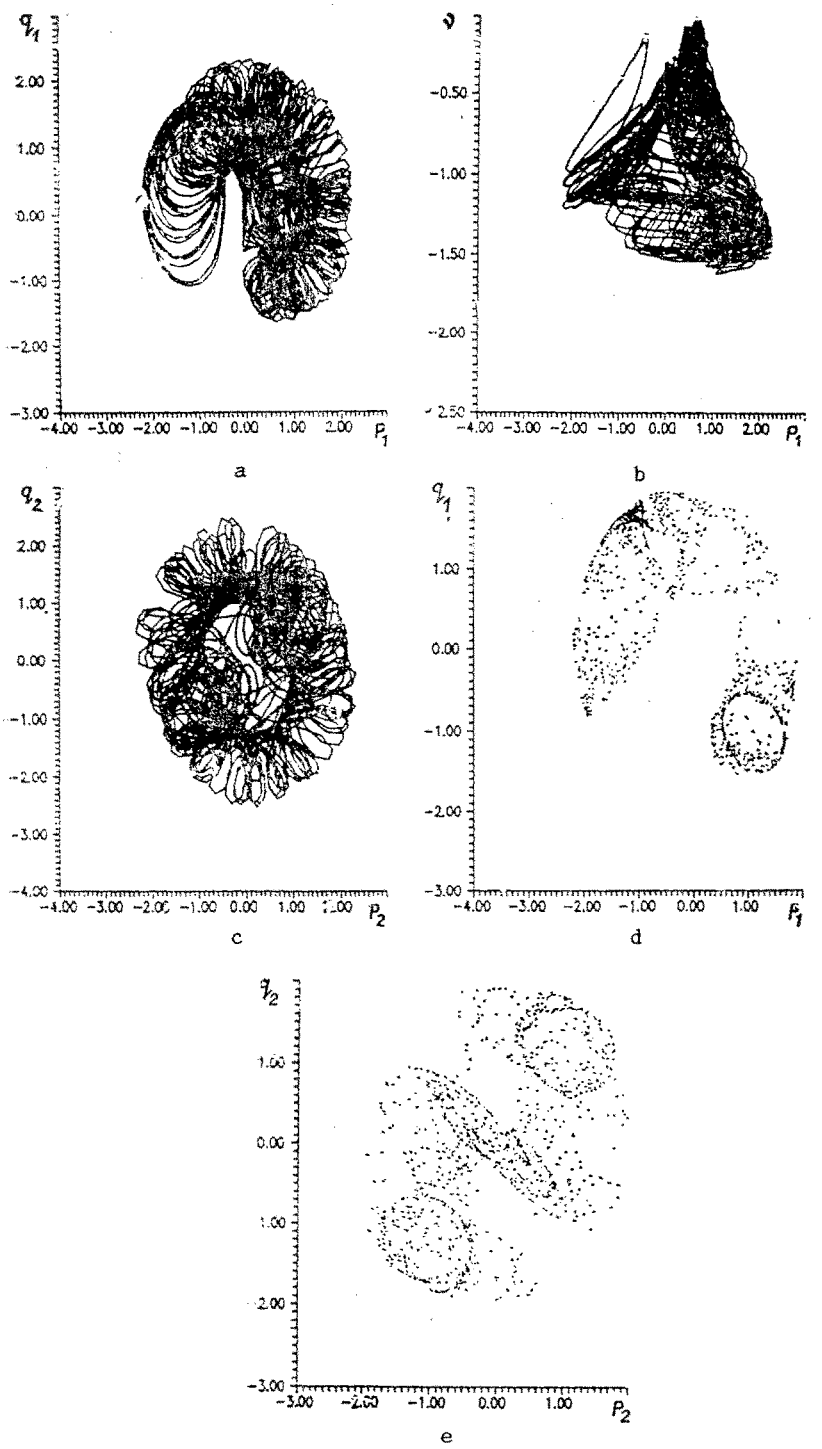

Fig. 5

For $N_1 = 0.38001$ the chaotic attractor vanishes, and a limiting cycle of period 8.75 is generated in the system, which then changes by a limiting cycle of period 4.375, and then by a stable equilibrium position (see Table 1). Thus, the study of steady-state regimes of motion in system (15) has demonstrated a substantial difference of not only the types of these motions (stationary, periodic, and chaotic), but also a different structure and flow in one class — the chaotic one. In this case we succeeded in separating a region of parameters, a most critical region, where "large" chaos is realized, and where the breakdown is possible of stability and reliability criteria of the functioning of the mechanical system.

LITERATURE CITED

1. V. O. Kononenko, Vibrational Systems with Bounded Excitations [in Russian], Nauka, Moscow (1964).

2. T. S. Krasnopol'skaya and A. Yu. Shvets, "Regular and chaotic surface waves in fluids with bounded excitation of oscillations of a cylindrical basin," Prikl. Mekh., 26, No. 8, 85-93 (1990).
3. B. I. Rabinovich, Introduction to Dynamics of Rocket-Carrier Space Apparatus [in Russian], Mashinostroenie, Moscow (1983).
4. G. B. Whitham, Linear and Nonlinear Waves, Wiley, New York (1974).
5. G. Benettin, L. Galgani, and J. M. Strelcyn, "Kolmogorov entropy and numerical experiments," Phys. Rev. A, 14, No. 6, 2238-2342 (1976).
6. M. Henon, "On the numerical computation of Poincaré maps," Physica, D5, No. 2 (1982).
7. J. W. Miles, "Nonlinear surface waves in closed basins," J. Fluid Mech., 75, Part 3, 419-448 (1976).
8. J. W. Miles, "Internally resonant surface waves in a circular cylinder," J. Fluid Mech., 149, Part 1, 1-14 (1984).
9. J. W. Miles, "Resonantly forced surface waves in a circular cylinder," J. Fluid. Mech., 149, Part 1, 15-31 (1984).

INDUCED OSCILLATION OF A VISCOELASTIC PLATE, TAKING ACCOUNT OF HEAT LIBERATION

I. A. Kiiko and S. Yu. Gvozdev

UDC 539.3

In solving coupled thermoviscoelasticity problems – in particular, for the induced nonlinear oscillations of plates and shells – numerical methods have mostly been used; analytical approaches have not been adequately developed. Although analytical approaches are approximate in all the problems considered, their importance is obvious: they permit judgements regarding the qualitative behavior of structures. Therefore, the aim of the present work is the correct formulation and approximate analytical solution of the thermoviscoelasticity problem for the induced oscillations of a rectangular plate made of a linear viscoelastic material, taking account of the internal heat liberation, and investigation of the influence of temperature and geometric nonlinearity on the characteristics of induced oscillation. Suppose that a plate occupying the region $0 \leq x \leq a$, $0 \leq y \leq b$ in the XOY plane undergoes oscillations under the action of a transverse load of intensity $q = F \sin \omega t$ varying harmonically over time. The plate surface is assumed to be heat insulated, and a constant temperature T_0 is maintained at its ends.

The system of equations describing the motion of a viscoplastic plate consists of the Karman equation, in which the elastic modulus E is replaced by its operator analog $\check{E}$, and the heat-conduction equation

$$\begin{cases} \dfrac{D_0}{E_0 h}\check{E}\nabla^4 w = L(w;\ \Phi) - \rho\dfrac{\partial^2 w}{\partial t^2} + \dfrac{q}{h}; \\ \nabla^4\Phi = -\check{E}L_1(w;\ w). \\ c\dfrac{\partial T}{\partial t} - \lambda\Delta T = s_{ij}^z \dot{e}_{ij}^z - \dfrac{s_{ij}^z \dot{s}_{ij}^z}{R(0)} + 3\sigma^z\dot{\varepsilon}^z - \dfrac{\sigma^z\dot{\sigma}^z}{R_1(0)} \\ \check{E}[\varphi(t)] = E_0[1 - \varepsilon_1\theta(x, y, z, t)]\left[\varphi(t) - \int_0^t \Gamma(t-\tau, T)\,\varphi(\tau)\,d\tau\right]. \end{cases} \tag{1}$$

Here E_0 is the instantaneous elastic modulus; $D_0 = E_0 h^3/12(1-\nu^2)$ is the corresponding cylindrical rigidity; ν is Poisson's ratio (assumed to be constant); h is the plate thickness and w is its flexure; ρ and $\Gamma(t, T)$ are the density and relaxational kernel of the plate material; Φ is the stress function; $L(w, \Phi)$ and $L_1(w, w)$ are the operators known from plate theory [1]; c and λ are the specific heat and thermal conductivity of the material, respec-

Moscow Automechanics Institute. Translated from Prikladnaya Mekhanika, Vol. 28, No. 6, pp. 61-66, June, 1992. Original article submitted January 25, 1990.

 1063-7095/92/2806-0394$12.50